

## Article

# Digital Detection of Olive Oil Rancidity Levels and Aroma Profiles Using Near-Infrared Spectroscopy, a Low-Cost Electronic Nose and Machine Learning Modelling

Claudia Gonzalez Viejo <sup>\*</sup> and Sigfredo Fuentes 

Digital Agriculture, Food and Wine Group, School of Agriculture and Food, Faculty of Veterinary and Agricultural Sciences, The University of Melbourne, Parkville, VIC 3010, Australia; sfuentes@unimelb.edu.au

\* Correspondence: cgonzalez2@unimelb.edu.au

**Abstract:** The success of the olive oil industry depends on provenance and quality-trait consistency affecting the consumers' acceptability/preference and purchase intention. Companies rely on laboratories to analyze samples to assess consistency within the production chain, which may be time-consuming, cost-restrictive, and untimely obtaining results, making the process more reactive than predictive. This study proposed implementing digital technologies using near-infrared spectroscopy (NIR) and a novel low-cost e-nose to assess the level of rancidity and aromas in commercial extra-virgin olive oil. Four different olive oils were spiked with three rancidity levels (N = 17). These samples were evaluated using gas-chromatography-mass-spectroscopy, NIR, and an e-nose. Four machine learning models were developed to classify olive oil types and rancidity (Model 1: NIR inputs; Model 2: e-nose inputs) and predict the peak area of 16 aromas (Model 3: NIR; Model 4: e-nose inputs). The results showed high accuracies (Models 1–2: 97% and 87%; Models 3–4: R = 0.96 and 0.93). These digital technologies may change companies from a reactive to a more predictive production of food/beverages to secure product quality and acceptability.

**Keywords:** olive oil faults; artificial intelligence; digital sensors; artificial neural networks; GC-MS



**Citation:** Gonzalez Viejo, C.; Fuentes, S. Digital Detection of Olive Oil Rancidity Levels and Aroma Profiles Using Near-Infrared Spectroscopy, a Low-Cost Electronic Nose and Machine Learning Modelling.

*Chemosensors* **2022**, *10*, 159.

<https://doi.org/10.3390/chemosensors10050159>

Academic Editors: Larisa Lvova, Alisa Rudnitskaya and Federico Marini

Received: 7 April 2022

Accepted: 25 April 2022

Published: 26 April 2022

**Publisher's Note:** MDPI stays neutral with regard to jurisdictional claims in published maps and institutional affiliations.



**Copyright:** © 2022 by the authors. Licensee MDPI, Basel, Switzerland. This article is an open access article distributed under the terms and conditions of the Creative Commons Attribution (CC BY) license (<https://creativecommons.org/licenses/by/4.0/>).

## 1. Introduction

Olive oil is highly consumed globally, with 3.1 million metric tons in 2020–2021 [1]. Its popularity is mainly due to its characteristic flavor, aroma, and health benefits. It mainly contains oleic acid, a monounsaturated fatty acid responsible for decreasing cardiovascular diseases, strokes, and mortality rates [2,3]. However, it may have shelf-life issues due to inadequate packaging, transportation, and storage, which may produce the formation of hydroperoxides due to oxidation of fatty acids when in contact with light, high temperatures, and oxygen [4]. These hydroperoxides cause the formation of different volatile compounds, which are responsible for off-aromas and off-flavors due to rancidity in olive oil, which negatively alters its sensory descriptors and, therefore, affects the product's quality and consumer acceptability [5–7].

The traditional and most common methods to analyze aromas and rancidity in olive oil consist of the use of (i) gas chromatography-mass spectroscopy (GC-MS) with headspace solid-phase microextraction (SPME) to assess the different volatile aromatic compounds [5,8,9]; (ii) evaluation of peroxide value through infrared or mass spectrometry [10], or (iii) combined techniques of GC, and descriptive sensory analysis with trained panelists to assess sensory descriptors related to aromas and flavors including rancidity and their intensity [5,8,11]. However, the first two methods require a specialized laboratory with enough space to place the equipment, which is costly. All three methods are time-consuming and require very well-trained personnel to operate the equipment, conduct the sensory sessions, and perform and interpret the statistical analyses. Olive oil companies, especially small to medium-sized, can only resort to sending samples to these laboratories

in order to obtain very detailed reports from those samples. However, they are costly, and reports may take several days or weeks to arrive, considering the workload from those laboratories, making these procedures impractical.

To overcome these issues, other methods have been developed to assess the chemical fingerprint and identify the presence of compounds, such as aromas and fatty acids with near-infrared (NIR) spectroscopy, and to assess aromas and rancidity in olive oils that consist of using electronic noses (e-noses), which are constructed using an integration of different digital gas sensors. Christy et al. [12] used NIR within the 833–2500 nm range to measure transmittance and analyzed with partial least squares (PLS) models to assess olive oil samples and identify adulteration with a very high correlation coefficient ( $R = 0.99$ ). Milinovic et al. [13] assessed olive oil samples using Fourier transform NIR (800–2220 nm) and developed several PLS models obtaining high accuracy to predict different fatty acids  $R > 0.85$ . Savarese et al. [5] used a commercial e-nose to monitor the development of rancidity of virgin olive oils during storage using statistical analyses, the principal components analysis that was able to visibly separate samples according to rancidity level, and correlation analysis against sensory rancidity rating obtaining a low-moderate determination coefficient  $R^2 = 0.64$ . Aparicio et al. [8] also used a commercial e-nose to assess rancidity in virgin olive oils; the authors applied a non-linear regression equation obtained from a regression on principal components; however, this study did not report any statistical values to assess the accuracy of predictions or separation of samples. Lerma-Garcia et al. [14] used a commercial e-nose to predict defects in sunflower oils using artificial neural networks, obtaining accuracies within 75–85% for the testing stage. Furthermore, Cano Marchal et al. [15] used a commercial e-nose coupled with logistic regression to predict the intensity of fruity aroma in virgin olive oil with 88% accuracy. However, these studies have been conducted using commercial e-noses, which are expensive and not portable; therefore, in these studies remain the issues regarding the need for laboratory space and specialized personnel.

This study aimed to develop a novel method to assess the type of olive oil and level of rancidity as well as the peak area of volatile aromatic compounds (targets) using near-infrared spectroscopy (NIR) and a low-cost and portable e-nose as inputs with machine learning modeling that the olive oil industry can apply to obtain results in real-time about levels of rancidity and aroma profiles.

## 2. Materials and Methods

### 2.1. Samples Description

Four different Australian commercial extra virgin olive oil samples labeled as (i) light flavor, (ii) medium strength or classic flavor, (iii) strong or robust flavor, and (iv) first cold press were spiked with rancid oil provided by the same commercial company at three different levels (15%, 25%, and 50% of rancid oil). Additionally, a control sample of each olive oil plus one for rancid oil were used. All samples were measured in triplicates.

### 2.2. Gas Chromatography/Mass Spectroscopy

Samples were analyzed using a gas chromatograph with the 5977B mass selective detector (Agilent Technologies, Inc., Santa Clara, CA, USA) (detection limit: 1.5 fg). This equipment was integrated with a PAL3 autosampler system (CTC Analytics AG, Zwingen, Switzerland). An HP-5MS column (Agilent Technologies, Inc., Santa Clara, CA, USA; length: 30 m, inner diameter: 0.25 mm, and film: 0.25  $\mu$ ) was used, and the carrier gas was helium at 1 mL  $\text{min}^{-1}$  flow rate. As described by Gonzalez Viejo et al. (2019), this method used headspace SPME. A blank sample was used at the start to confirm no carryover from prior measurements. Compounds were identified using the National Institute of Standards and Technology (NIST; National Institute of Standards and Technology, Gaithersburg, MD, USA) library.

### 2.3. Near-Infrared Spectroscopy

Three measurements were taken for each replicate of each sample using a hand-held NIR spectroscopy device (MicroPHAZIR RX Analyzer; Thermo Fisher, Waltham, MA, USA) within the 1596–2396 nm range. The analysis was performed as described by Gonzalez Viejo et al. [16]. For this, a filter paper Whatman<sup>®</sup> qualitative filter paper, Grade 1 (diameter 55 mm; Whatman, plc., Maidstone, UK), was used to absorb the olive oil sample and measure the chemical fingerprint by further subtracting the absorbance values of the dry filter paper. The first derivative of the absorbance values was obtained using Savitzky–Golay polynomial order two with Unscrambler<sup>®</sup> X ver. 10.3 (CAMO Software, Oslo, Norway). Both the raw signal and first derivative were plotted to enhance the overtones.

### 2.4. Electronic Nose

A low-cost e-nose consisting of an array of nine different gas sensors was used to measure the voltage values [17] of all samples and treatments in triplicates. These sensors are sensitive to different gases such as (i) alcohol (MQ3), (ii) methane (MQ4), (iii) carbon monoxide (MQ7), (iv) hydrogen (MQ8), (v) ammonia, alcohol, and benzene (MQ135), (vi) hydrogen sulfide (MQ136), (vii) ammonia (MQ137), (viii) benzene, alcohol, and ammonia (MQ138), and (ix) carbon dioxide (MG811). The raw signal was analyzed using a Matlab<sup>®</sup> R2021a (Mathworks, Inc., Natick, MA, USA) code developed by the Digital Agriculture, Food and Wine group from The University of Melbourne (DAFW-UoM) to divide the peak area of the curve into 10 subsections and calculate 10 mean values [18]. The MQ136 sensor was removed for all analysis as hydrogen sulfide was not detected in any sample. Data analysis was conducted using the raw signal of the e-nose rather than the values of the specific gases since some sensors are also sensitive to other gases.

### 2.5. Statistical Analysis and Machine Learning Modeling

The e-nose data were analyzed using ANOVA to assess significant differences between samples with Tukey's honest significant difference (HSD) as a *post hoc* test ( $\alpha = 0.05$ ) with XLSTAT ver. 2020.3.1 (Addinsoft, New York, NY, USA). Furthermore, a correlation matrix was constructed using Matlab<sup>®</sup> 2021a to assess significant correlations ( $p < 0.05$ ) between the volatile aromatic compounds measured with GC-MS and the e-nose.

Two artificial neural network (ANN) classification models were developed using a code written in Matlab<sup>®</sup> R2021a by the DAFW-UoM group. The absorbance values measured with NIR (Model 1) and the e-nose outputs (Model 2) were used as inputs to classify samples into the type of olive oil and level of rancidity, including a rancid control with a total of 17 categories (Figure 1A). From 17 different ANN training algorithms tested [19], Bayesian Regularization provided the best Model 1 and Scaled Conjugate Gradient Model 2 with high accuracy and good performance with no under- or overfitting assessed by comparing the mean squared error (MSE; Model 1) or cross-entropy (Model 2) values of each stage. Lower training MSE or cross-entropy than testing and similar validation and testing values indicate no under- or overfitting. Samples were divided randomly as 70% training and 30% testing for Model 1, and 70% training, 15% validation, and 15% testing for Model 2 (Figure 1A).

Two ANN regression models were developed using another code written in Matlab<sup>®</sup> R2021a by the DAFW-UoM group. The NIR absorbance values (Model 3) and the e-nose outputs (Model 4) were used as inputs to predict the peak area of 16 different volatile aromatic compounds measured with GC-MS (Figure 1B). A total of 17 different ANN training algorithms were tested automatically, with Levenberg–Marquardt resulting in the best algorithm for Model 3 and Bayesian Regularization for Model 4, both using MSE to assess performance. Samples were divided randomly as 70% training, 15% validation, and 15% testing for Model 3, and 70% training and 30% testing for Model 4 (Figure 1B). After testing different numbers of neurons or neuron trimming (3, 5, 7, and 10), 10 resulted in the best and most efficient number for the four models.

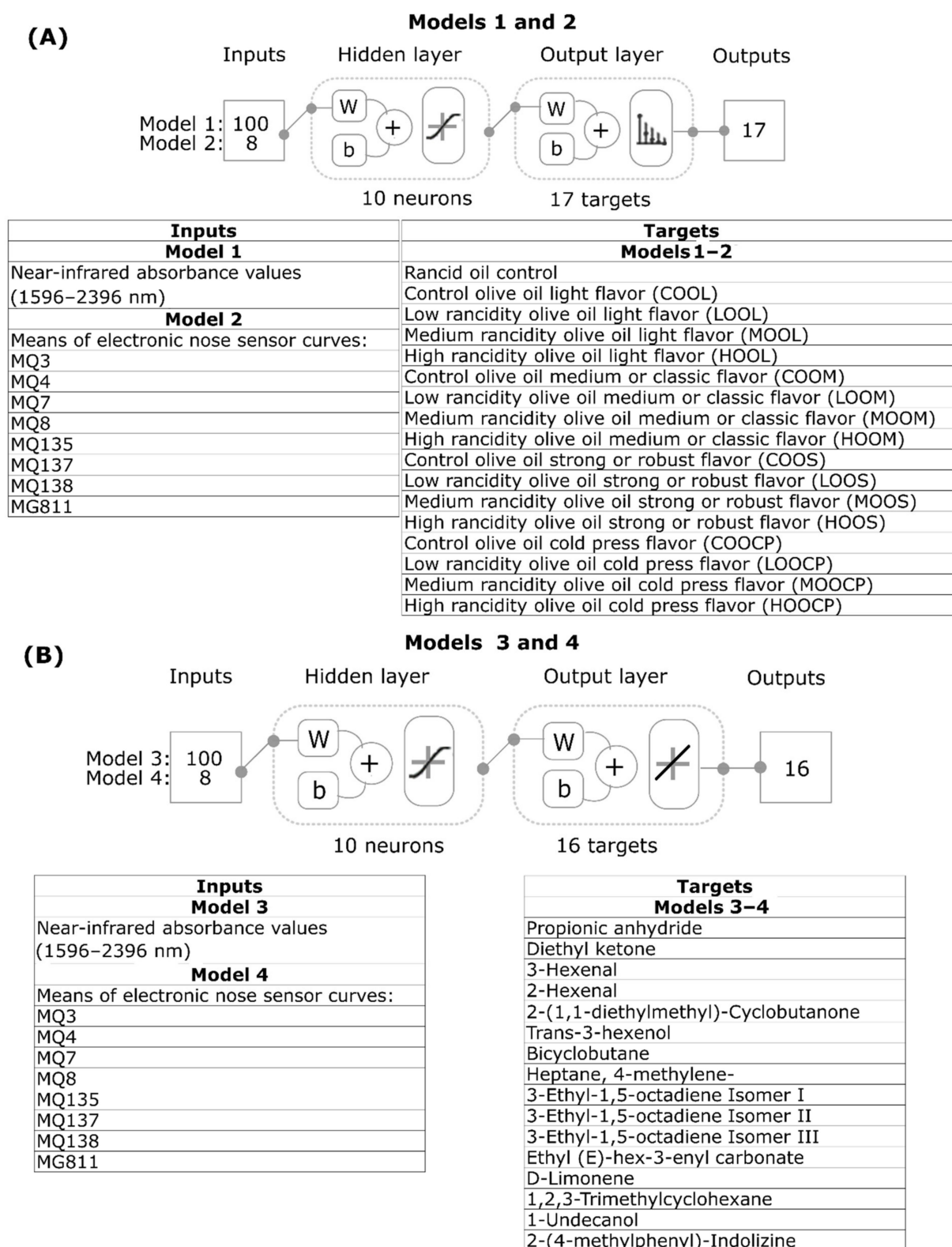


**Figure 1.** Artificial neural network models for (A) classification (Models 1 and 2), and (B) regression (Models 3 and 4), showing the inputs, targets/outputs, and number of neurons used for each.

### 3. Results and Discussion

#### 3.1. Volatile Aromatic Compounds from GC-MS

Table 1 shows that 16 volatile aromatic compounds that belong to nine main functional groups were found in the olive oil samples. Table S1 in Supplementary Material shows the peak area of the compounds for each sample and treatment. It can be observed that in the rancid oil control, only 2-(4-methylphenyl)-Indolizine was detected. D-limonene was only detected in the cold press olive oil, while heptane, 4-methylene- and at least one isomer of 3-Ethyl-1,5-octadiene were found in all olive oil samples and treatments. It was also found that all treatments had different compounds and/or peak areas compared to the controls, showing that the rancidity has altered the aroma of the sampled olive oils. Compounds such as 3-hexenal, 2-hexenal, different isomers of 3-Ethyl-1,5-octadiene, and D-limonene were also found in Portuguese [20] and Turkish olive oils [21]. Trans-3-hexenol has also been detected in olive oil by other authors [22,23]. It can be observed that the associated aromas are mainly related to green, floral, fruity, and musty, which are expected in commercial olive oils.

**Table 1.** Volatile aromatic compounds in olive oils detected using gas-chromatography-mass-spectroscopy and the associated aromas.

| Volatile Aromatic Compound          | Functional Group       | Aroma *                        |
|-------------------------------------|------------------------|--------------------------------|
| Propionic anhydride                 | Anhydride              | Pungent                        |
| Diethyl ketone                      | Ketone                 | Ethereal/Acetone               |
| 3-Hexenal                           | Aldehyde               | Green/Leafy/Apple/Melon        |
| 2-Hexenal                           | Aldehyde               | Green/Almond/Leafy/Apple/Plum  |
| 2-(1,1-dimethylethyl)-Cyclobutanone | Cyclic Ketone          | NR                             |
| Trans-3-hexenol                     | Alcohol                | Green/Leafy/Floral/Oily/Earthy |
| Bicyclobutane                       | Cycloalkane            | NR                             |
| Heptane, 4-methylene-               | Hydrocarbon/Alkene     | NR                             |
| 3-Ethyl-1,5-octadiene Isomer I      | Hydrocarbons/Alkadiene | Musty                          |
| 3-Ethyl-1,5-octadiene Isomer II     | Hydrocarbons/Alkadiene | Musty                          |
| 3-Ethyl-1,5-octadiene Isomer III    | Hydrocarbons/Alkadiene | Musty                          |
| Ethyl (E)-hex-3-enyl carbonate      | Carbonate ester        | NR                             |
| D-Limonene                          | Monoterpene            | Citrus/Orange/Fresh/Sweet      |
| 1,2,3-Trimethylcyclohexane          | Cycloalkane            | NR                             |
| 1-Undecanol                         | Alcohol                | Waxy/Fresh/Rose/Soapy/Citrus   |
| 2-(4-methylphenyl)-Indolizine       | Heterocyclic aromatic  | NR                             |

\* Associated aromas were obtained from The Good Scents Company [24] and da Costa et al. [25]. Abbreviations: NR: not reported.

#### 3.2. Near-Infrared Spectroscopy

Figure 2 shows that most overtones were found within the 1600–1800 nm and 2100–2396 nm ranges; these can be found within both the raw signal (Figure 2A) and the enhanced peaks using the first derivative (Figure 2B). For the main overtones, compounds such as aliphatic hydrocarbons (1699–1700, 1732, 1767, and 2323 nm), ketones, and compounds with a methyl group (1700 nm), alcohols (1737 nm), aromatic hydrocarbons (1749 nm) were found [26]. As shown in Table 1, aromas with functional groups such as ketones, hydrocarbons, and alcohols were detected with GC-MS, which shows that NIR could also detect their presence. Milinovic et al. [13] also found overtones within the 1727–1761 nm range; other authors [27] reported the presence of oleic acid at 1725 nm, which was also detected in the samples used in the present study. Furthermore, other overtones can be observed for polysaccharides (2278, 2285, 2340, and 2357 nm),

aryl (2299 and 2392 nm), and, as expected, lipids and oils (2140–2145, 2310–2315, and 2380–2385 nm) [26,28]. Other studies have also reported overtones around 2300 nm in olive oil samples [29]. These results evidence the broad presence of aliphatic hydrocarbons as several overtones that correspond to these compounds were found; these are naturally present in olive oil but may also be due to contamination with mineral oils [30–32]. In Figure 2B, it can be observed that for most of the overtones from these compounds, the high rancidity olive oil cold press (HOOCP) sample had the highest absorbance.

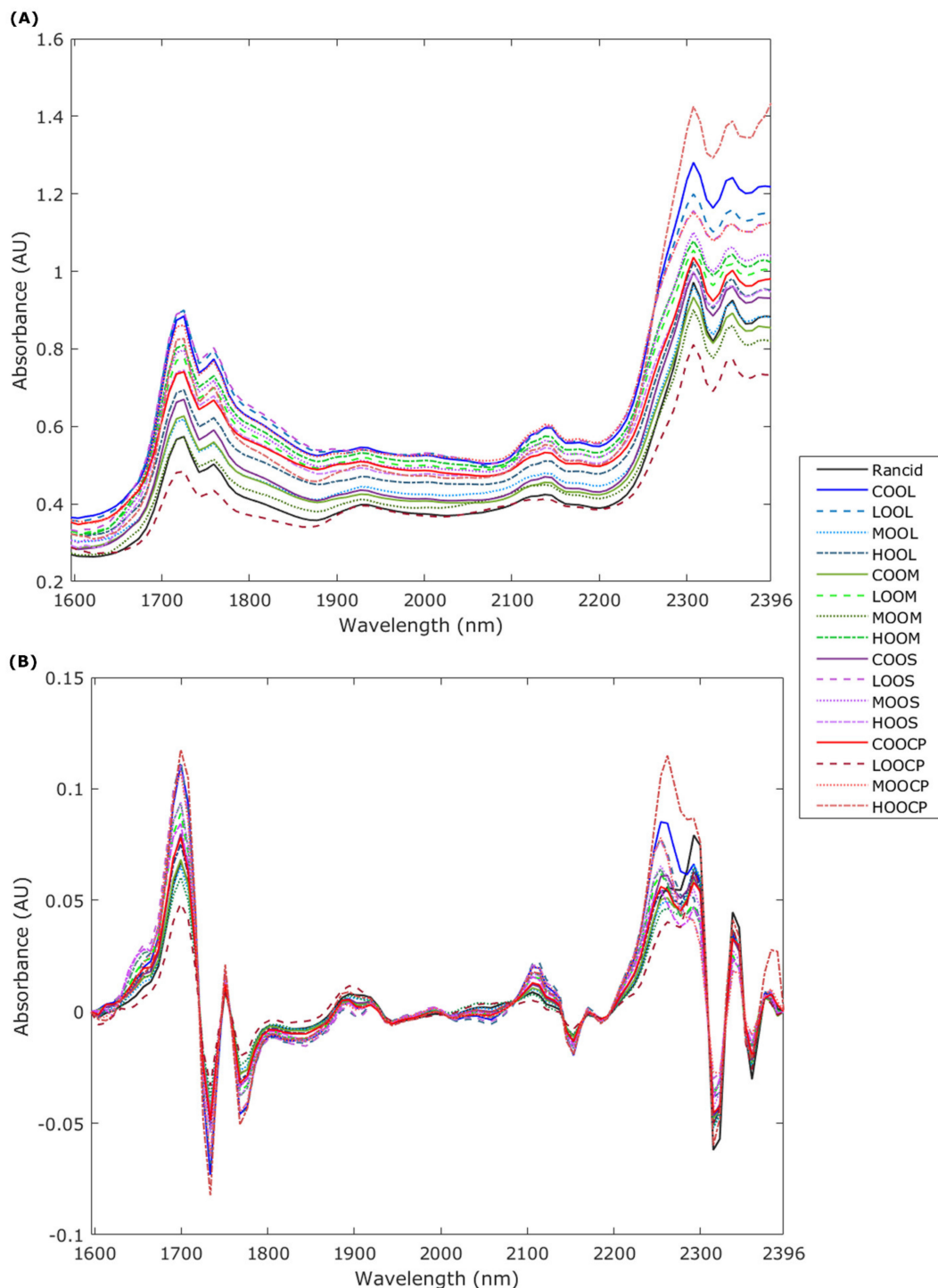


**Figure 2.** Chemical fingerprinting from near-infrared spectroscopy (1596–2396 nm) using (A) the raw signal and (B) the Savitzky–Golay first derivative.

### 3.3. Electronic Nose

Figure 3 shows significant differences ( $p < 0.05$ ) between samples for all e-nose sensors used in this study. Considering that the MG811 sensor signal is inverse (higher voltage, lower concentration), carbon dioxide presented the lowest concentration. Therefore, the MQ4 sensor, which is sensitive to methane and to a lower extent to alcohol, and smoke, was the highest in voltage, with the rancid oil control significantly higher than the other samples and treatments. The presence of methane in oil may be explained since this is a by-product of oil production [33], while the alcohols, as shown in the GC-MS and NIR results and as reported in other studies [34], are commonly present in commercial olive oil, including the samples analyzed in the present study. It can also be observed that the medium and high rancidity cold press olive oil samples (MOOCP and HOOCP) showed the highest raw signals related to alcohol concentration (MQ3).

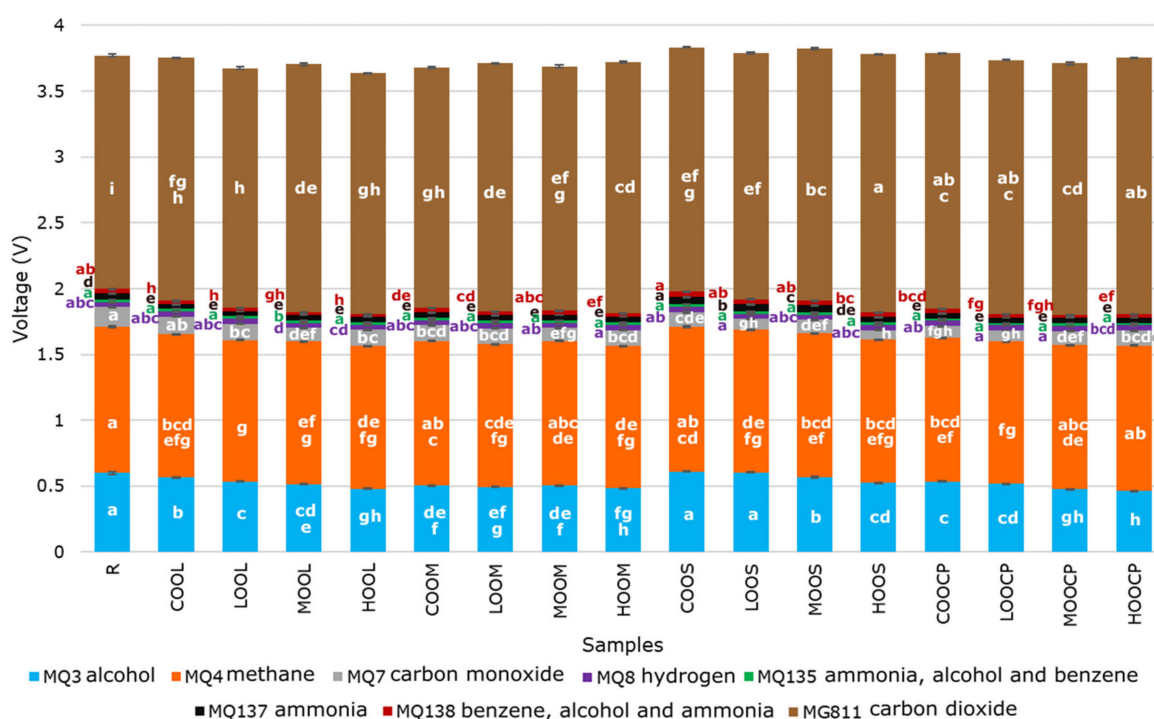


**Figure 3.** Stacked bars graph with mean values of the electronic nose outputs. Error bars depict the standard error. Different letters (a–i) represent significant differences between samples based on the least significant difference (LSD) *post hoc* test ( $p < 0.05$ ). Abbreviations: R: Rancid; C: Control; OO: Olive oil; L at the start: Low; L at the end: Light; M at the start: Medium; M at the end: medium strength or classic flavor; H: High; S: strong or robust flavor; CP: cold press.

### 3.4. Correlations between Volatile Aromatic Compounds (GC-MS) and E-Nose Gas Sensors

Figure 4 shows that MQ3 sensor (alcohol) has a significant ( $p < 0.05$ ) and positive correlation with 2-hexenal ( $r = 0.58$ ), bicyclobutane ( $r = 0.42$ ), heptane, 4-methylene- ( $r = 0.49$ ), 3-ethyl-1,5-octadiene Isomers I, II and III ( $r = 0.32$ ,  $0.28$  and  $0.51$ , respectively), and negative correlation with trans-3-hexenol ( $r = -0.58$ ), and ethyl (E)-hex-3-enyl carbonate ( $r = -0.40$ ). On the other hand, MQ137 (ammonia) and MQ138 (benzene, alcohol and ammonia) were positively correlated with 2-hexenal ( $r = 0.70$  and  $0.41$ , respectively), bicyclobutane ( $r = 0.59$  and  $0.35$ , respectively), heptane, 4-methylene- ( $r = 0.71$  and  $0.42$ , respectively), 3-Ethyl-1,5-octadiene Isomer III ( $r = 0.50$ , and  $0.29$ , respectively), and negatively correlated with trans-3-hexenol ( $r = -0.58$ , and  $-0.51$ , respectively) and ethyl (E)-hex-3-enyl carbonate ( $r = -0.56$ , and  $-0.46$ , respectively). The correlations found between the e-nose and aromatic volatile compounds analyzed with GC-MS showed that e-nose responses would be good predictors of the aromatic compounds from GC-MS, which was demonstrated

in the following subsection for machine learning modelling. Hence, from a parametric engineering point of view, all sensors integrated in the e-nose were considered for machine-learning modeling.

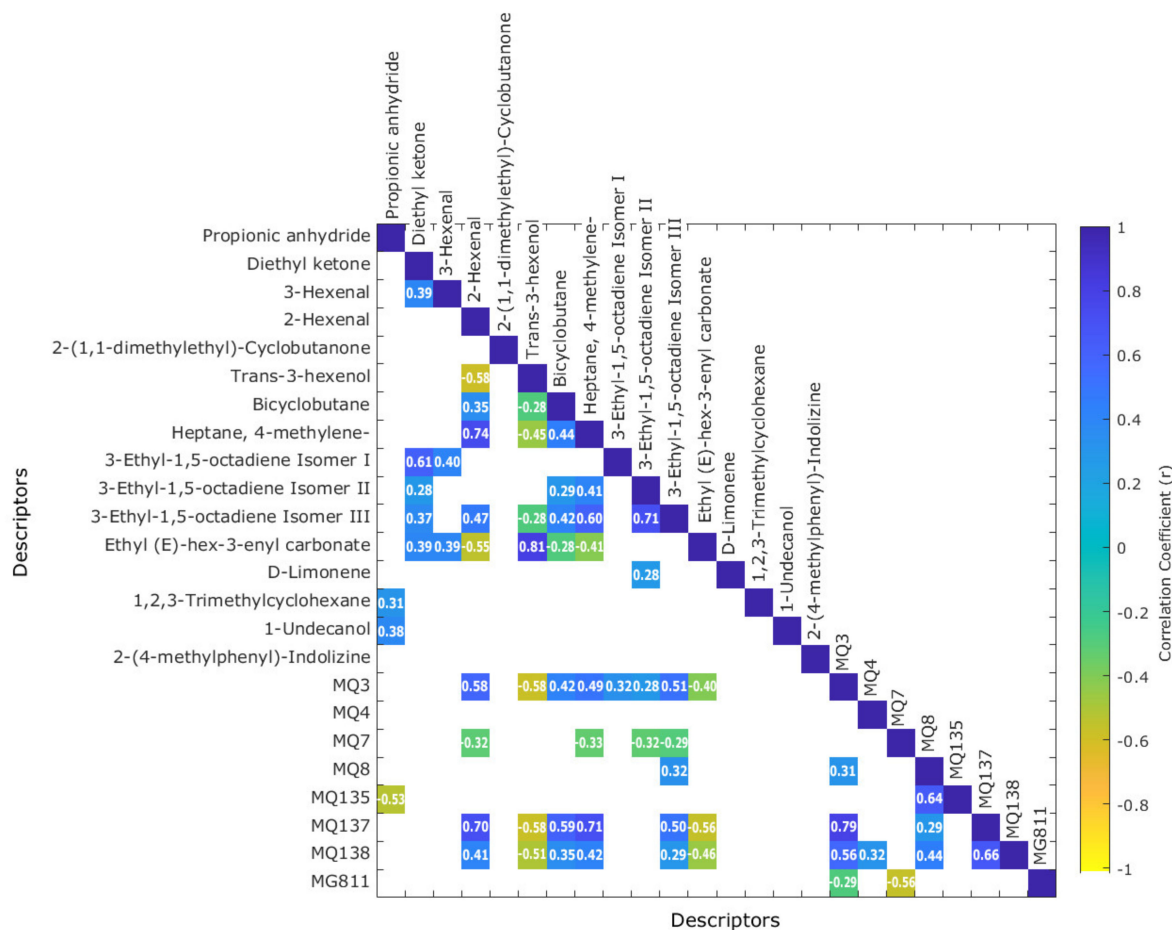


**Figure 4.** Matrix showing significant correlations ( $p < 0.05$ ) between the volatile aromatic compounds and e-nose gas sensors. Abbreviations: MQ3: alcohol; MQ4: methane; MQ7: carbon monoxide; MQ8: hydrogen; MQ135: ammonia, alcohol, and benzene; MQ137: ammonia; MQ138: benzene, alcohol, and ammonia; MG811: carbon dioxide.

### 3.5. Machine Learning Modelling

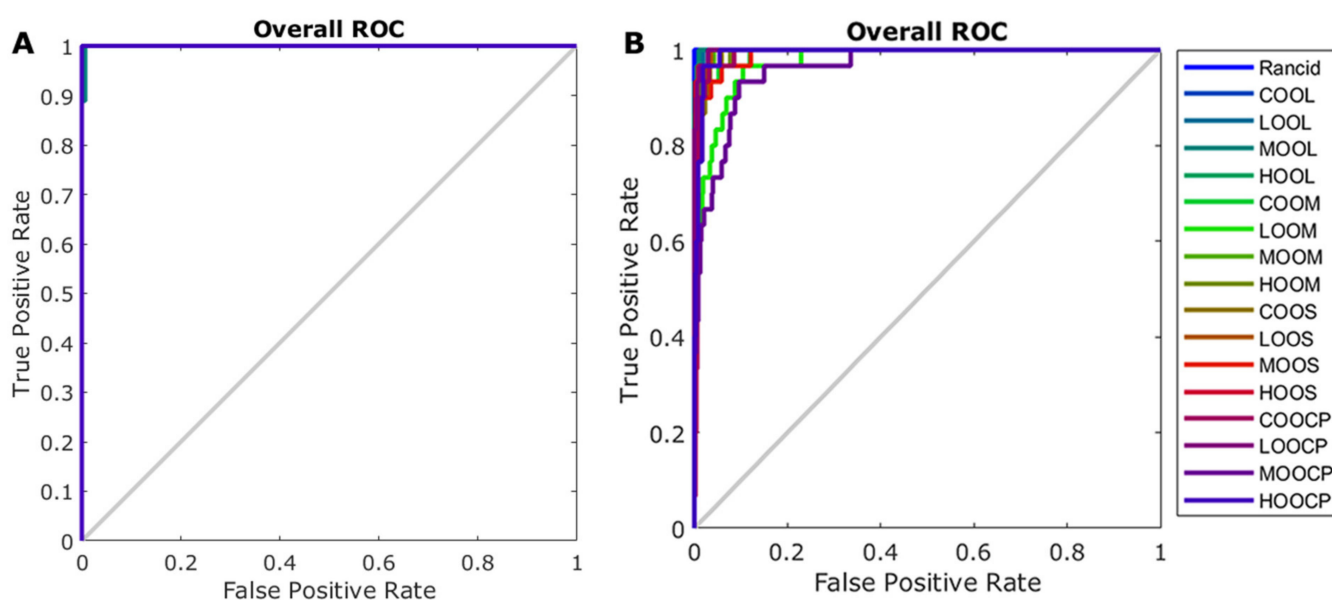
Table 2 shows that Model 1 had very high accuracy (97%) in classifying samples into the different olive oils and rancidity treatments using the NIR absorbance values as inputs, while Model 2 used e-nose raw voltage values as inputs and had an accuracy of 87%. Even though Model 2 had lower accuracy than Model 1, it is a great option to use as a low-cost, portable, reliable, non-destructive, and rapid method to assess the type of olive oil and presence/level of rancidity.

Figure 5 shows the receiver operating characteristics curves of Models 1 (Figure 5A) and 2 (Figure 5B). It can be observed that in Model 1, developed using NIR absorbance values as inputs, most of the samples were close to the true-positive rate (sensitivity), with the MOOCP class being the highest misclassified category (sensitivity: 0.67; precision: 1.00) followed by MOOL (sensitivity: 0.89; precision: 0.69) and all other categories with both sensitivity and precision of 1.00. On the other hand, Model 2, developed using the e-nose outputs as inputs, also had results rates close to the true-positive rate, with MOOCP as the highest in misclassification (sensitivity: 0.57; precision: 0.71) followed by LOOM (sensitivity: 0.67; precision: 0.74) and COOS (sensitivity: 0.73; precision: 0.88). This may be further improved by feeding the models with more samples.

**Table 2.** Accuracies and performance for Models 1 and 2 using artificial neural network pattern recognition.

| Stage  | Samples | Accuracy | Error | Performance<br>(Model 1: MSE;<br>Model 2:<br>Cross-Entropy) |
|--|---------|----------|-------|---|
| Model 1 Inputs: Near-infrared absorbance values (Classification) |         |          |       |   |
| Training   | 107     | 100%     | 0.0%  | <0.01   |
| Testing  | 46      | 91.3%    | 8.7%  | 0.01  |
| Overall  | 153     | 97.4%    | 2.6%  | -   |
| Model 2 Inputs: electronic nose voltage values (Classification)  |         |          |       |   |
| Training   | 356     | 89.0%    | 11.0% | 0.02  |
| Validation   | 77      | 79.2%    | 20.8% | 0.04  |
| Testing  | 77      | 81.8%    | 18.2% | 0.04  |
| Overall  | 510     | 86.5%    | 13.5% | -   |

Abbreviations: MSE: means squared error.



**Figure 5.** Receiver operating characteristics curves for (A) Model 1 developed using near-infrared spectroscopy absorbance values, and (B) Model 2 developed using electronic nose outputs as inputs. Abbreviations: R: Rancid; C: Control; OO: Olive oil; L at the start: Low; L at the end: Light; M at the start: Medium; M at the end: medium strength or classic flavor; H: High; S: strong or robust flavor; CP: cold press.

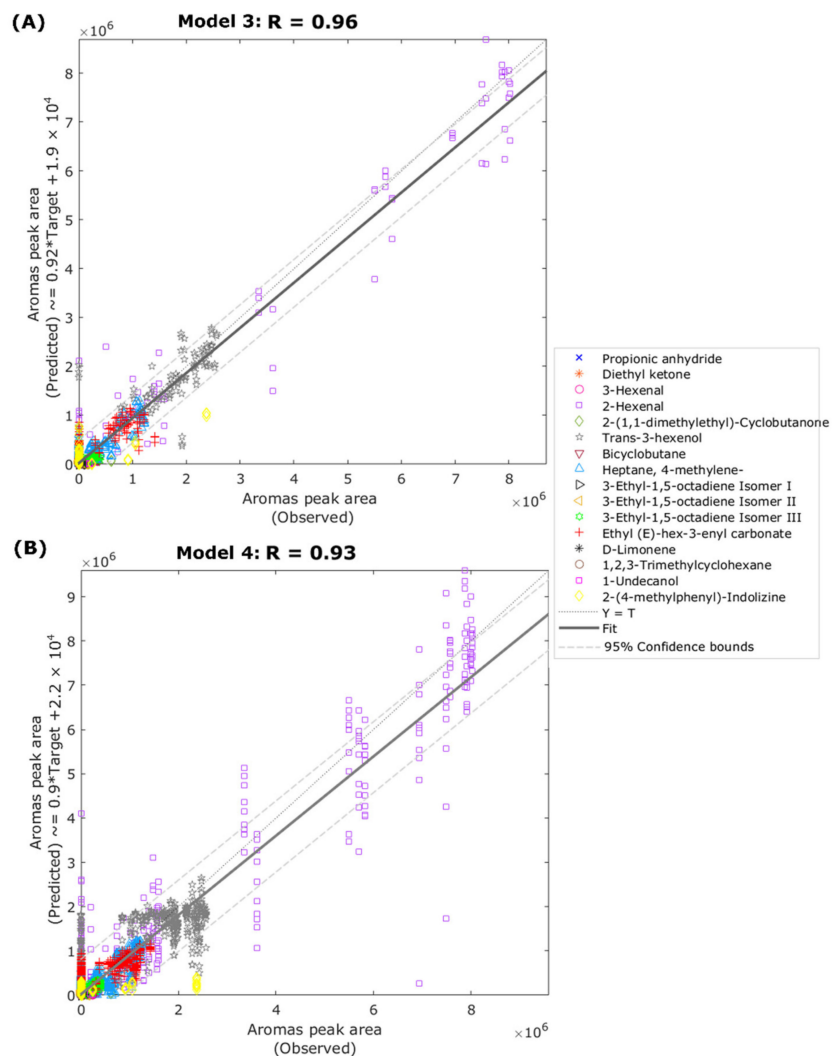
Table 3 shows that Models 3 and 4 had very high accuracies based on correlation coefficient ( $R = 0.96$  and  $0.93$ , respectively) and slope ( $b = 0.92$  and  $0.90$ , respectively) to predict the peak area of different volatile aromatic compounds. Considering the performance values as stated in materials and methods Section 2.5, none of the four models shown in Tables 2 and 3 presented any signs of under- or overfitting, making the models presented in this study robust and realistic.

Figure 6 shows the overall regression models; according to the 95% confidence bounds, it can be observed that Model 3 (Figure 6A) had 4.98% of outliers (122 out of 2448 data points), while Model 4 (Figure 6B) had 5% of outliers (408 out of 8160 data points).

**Table 3.** Correlation coefficients and performance for Models 3 and 4 using artificial neural network regression algorithms.

| Stage  | Samples | Observations | Correlation Coefficient (R) | Slope | Performance (MSE)      |
|--|---------|--------------|-----------------------------|-------|------------------------|
| Model 3 Inputs: Near-infrared absorbance values (Regression) |         |              |                             |       |                        |
| Training   | 107     | 1712         | 0.98                        | 0.96  | $2.29 \times 10^{10}$  |
| Validation   | 23      | 368          | 0.91                        | 0.89  | $13.83 \times 10^{10}$ |
| Testing  | 23      | 368          | 0.94                        | 0.84  | $12.69 \times 10^{10}$ |
| Overall  | 153     | 2448         | 0.96                        | 0.92  | -                      |
| Model 4 Inputs: electronic nose voltage values (Regression)  |         |              |                             |       |                        |
| Training   | 357     | 5712         | 0.95                        | 0.90  | $7.45 \times 10^{10}$  |
| Testing  | 153     | 2448         | 0.90                        | 0.88  | $16.98 \times 10^{10}$ |
| Overall  | 510     | 8160         | 0.93                        | 0.90  | -                      |

Abbreviations: MSE: means squared error.

**Figure 6.** Overall artificial neural network regression models developed with (A) the near-infrared absorbance values (Model 3) and (B) the electronic nose voltage values (Model 4) as inputs to predict the peak area of volatile aromatic compounds.

As mentioned in the introduction, other authors have published studies using NIR or e-nose coupled with different machine learning methods to assess fatty acids, rancidity, or defects in olive and sunflower oils; however, those studies presented models with accuracies within 64–88% [5,8,13–15]. Furthermore, the e-noses used in those studies were commercial, non-portable, and less affordable than the proposed e-nose in the present study.

All four models were highly accurate and could be used as rapid, non-destructive methods to assess the aromas and rancidity of olive oil. The NIR Models 1 and 3 had higher accuracy than the e-nose Models 2 and 4; this is because the NIR measures the chemical fingerprint of the samples, including lipids, aromas, carbohydrates, among others, while the e-nose measures only volatile compounds and despite being able to detect other gases, it has higher sensitivity to specific gases as described in Section 2.4. These two methods (NIR and e-nose) were compared as different approaches that can be used to detect rancidity levels and aromas. This is to provide different options, one based on a chemical fingerprint and the other on volatile gases, to the tools and resources that the olive oil industry has based on digital technologies and machine learning. The NIR device is more expensive than the e-nose; therefore, small companies may not afford the NIR; however, the e-nose is an affordable, reliable, portable, and convenient option, making it an adequate option for manufacturers to monitor quality. Further research may be conducted to develop similar models to assess samples at different production stages from the field to the final product. This would allow early detection of any faults or defects that may be corrected on time to avoid economic losses.

#### 4. Conclusions

Artificial intelligence (AI), consisting of the integration of low-cost digital sensor technologies, offer highly accurate tools to be applied in the food and beverage industries to assess in real-time different manufacturing processes and the detection/prediction of faults due to unforeseen factors by the industry. This study has shown that by using NIR and low-cost e-noses, AI may contribute significantly to the olive oil industry by predicting and avoiding off-flavors and aromas related to rancidity, which is one of the major problems for this industry within olive oil production, packaging, transport, and storage. Due to the low cost of the digital tools developed, food industries may be able to do management strategies to modify manufacturing processes that may result in taint and spoilage of products before making them available in the market. These predictions are extremely important for product positioning and maintaining quality and preference among consumers. Finally, these digital technologies can be coupled with AI to develop digital twin processes to detect procedures that may produce off-flavors and aromas before packaging.

**Supplementary Materials:** The following supporting information can be downloaded at: <https://www.mdpi.com/article/10.3390/chemosensors10050159/s1>, Table S1. Mean peak area  $\pm$  standard error of volatile aromatic compounds and their retention time (RT).

**Author Contributions:** Conceptualization, C.G.V. and S.F.; methodology, C.G.V. and S.F.; software, C.G.V. and S.F.; validation, C.G.V. and S.F.; formal analysis, C.G.V. and S.F.; investigation, C.G.V. and S.F.; data curation, C.G.V. and S.F.; writing—original draft preparation, C.G.V. and S.F.; writing—review and editing, C.G.V. and S.F.; visualization, C.G.V. and S.F. All authors have read and agreed to the published version of the manuscript.

**Funding:** This research received no external funding.

**Institutional Review Board Statement:** Not applicable.

**Informed Consent Statement:** Not applicable.

**Data Availability Statement:** Data and intellectual property belong to The University of Melbourne; any sharing needs to be evaluated and approved by the university.

**Acknowledgments:** The authors would like to acknowledge Ranjith R. Unnithan and Bryce Widdicombe from the School of Engineering, Department of Electrical and Electronic Engineering of The University of Melbourne for their collaboration in electronic nose development.

**Conflicts of Interest:** The authors declare no conflict of interest.

## References

1. Shahbandeh, M. Consumption of Olive Oil Worldwide from 2012/13 to 2020/21. Available online: <https://www-statista-com.eu1.proxy.openathens.net/statistics/940491/olive-oil-consumption-worldwide/#statisticContainer> (accessed on 8 February 2022).
2. Teres, S.; Barceló-Coblijn, G.; Benet, M.; Alvarez, R.; Bressani, R.; Halver, J.E.; Escriba, P. Oleic acid content is responsible for the reduction in blood pressure induced by olive oil. *Proc. Natl. Acad. Sci. USA* **2008**, *105*, 13811–13816. [CrossRef]
3. Schwingshackl, L.; Hoffmann, G. Monounsaturated fatty acids, olive oil and health status: A systematic review and meta-analysis of cohort studies. *Lipids Health Dis.* **2014**, *13*, 1–15. [CrossRef] [PubMed]
4. Piscopo, A.; Poiana, M. Packaging and storage of olive oil. In *Olive Germplasm—The Olive Cultivation, Table Olive and Olive Oil Industry in Italy*; InTechOpen: London, UK, 2012; pp. 201–222.
5. Savarese, M.; Caporaso, N.; Parisini, C.; Paduano, A.; De Marco, E.; Sacchi, R. Application of an electronic nose for the evaluation of rancidity and shelf life in virgin olive oil. In Proceedings of the Electronic International Interdisciplinary Conference, Virtual, 2–6 September 2013; pp. 361–366.
6. Harwood, J.; Aparicio, R. *Handbook of Olive Oil: Analysis and Properties*; Springer: Berlin/Heidelberg, Germany, 2000.
7. Gámbaro, A.; Ellis, A.C.; Raggio, L. Virgin olive oil acceptability in emerging olive oil-producing countries. *Food Nutr. Sci.* **2013**, *4*, 37230. [CrossRef]
8. Aparicio, R.; Morales, M.T.; García-González, D.L. Towards new analyses of aroma and volatiles to understand sensory perception of olive oil. *Eur. J. Lipid Sci. Technol.* **2012**, *114*, 1114–1125. [CrossRef]
9. Morales, M.; Rios, J.; Aparicio, R. Changes in the volatile composition of virgin olive oil during oxidation: Flavors and off-flavors. *J. Agric. Food Chem.* **1997**, *45*, 2666–2673. [CrossRef]
10. Barthel, G.; Grosch, W. Peroxide value determination—Comparison of some methods. *J. Am. Oil Chem. Soc.* **1974**, *51*, 540–544. [CrossRef]
11. Morales, M.; Luna, G.; Aparicio, R. Comparative study of virgin olive oil sensory defects. *Food Chem.* **2005**, *91*, 293–301. [CrossRef]
12. Christy, A.A.; Kasemsumran, S.; Du, Y.; Ozaki, Y. The detection and quantification of adulteration in olive oil by near-infrared spectroscopy and chemometrics. *Anal. Sci.* **2004**, *20*, 935–940. [CrossRef]
13. Milinovic, J.; Garcia, R.; Rato, A.E.; Cabrita, M.J. Rapid Assessment of Monovarietal Portuguese Extra Virgin Olive Oil's (EVOO's) Fatty Acids by Fourier-Transform Near-Infrared Spectroscopy (FT-NIRS). *Eur. J. Lipid Sci. Technol.* **2019**, *121*, 1800392. [CrossRef]
14. Lerma-García, M.; Cerretani, L.; Cevoli, C.; Simó-Alfonso, E.; Bendini, A.; Toschi, T.G. Use of electronic nose to determine defect percentage in oils. Comparison with sensory panel results. *Sens. Actuators B Chem.* **2010**, *147*, 283–289. [CrossRef]
15. Cano Marchal, P.; Sanmartin, C.; Satorres Martínez, S.; Gómez Ortega, J.; Mencarelli, F.; Gámez García, J. Prediction of fruity aroma intensity and defect presence in virgin olive oil using an electronic nose. *Sensors* **2021**, *21*, 2298. [CrossRef]
16. Gonzalez Viejo, C.; Fuentes, S.; Torrico, D.; Howell, K.; Dunshea, F. Assessment of beer quality based on foamability and chemical composition using computer vision algorithms, near infrared spectroscopy and machine learning algorithms. *J. Sci. Food Agric.* **2018**, *98*, 618–627. [CrossRef] [PubMed]
17. Gonzalez Viejo, C.; Fuentes, S.; Godbole, A.; Widdicombe, B.; Unnithan, R.R. Development of a low-cost e-nose to assess aroma profiles: An artificial intelligence application to assess beer quality. *Sens. Actuators B Chem.* **2020**, *308*, 127688. [CrossRef]
18. Gonzalez Viejo, C.; Tongson, E.; Fuentes, S. Integrating a Low-Cost Electronic Nose and Machine Learning Modelling to Assess Coffee Aroma Profile and Intensity. *Sensors* **2021**, *21*, 2016. [CrossRef] [PubMed]
19. Gonzalez Viejo, C.; Torrico, D.; Dunshea, F.; Fuentes, S. Development of Artificial Neural Network Models to Assess Beer Acceptability Based on Sensory Properties Using a Robotic Pourer: A Comparative Model Approach to Achieve an Artificial Intelligence System. *Beverages* **2019**, *5*, 33. [CrossRef]
20. Martins, N.; Jiménez-Morillo, N.T.; Freitas, F.; Garcia, R.; Da Silva, M.G.; Cabrita, M.J. Revisiting 3D van Krevelen diagrams as a tool for the visualization of volatile profile of varietal olive oils from Alentejo region, Portugal. *Talanta* **2020**, *207*, 120276. [CrossRef] [PubMed]
21. Kaftan, A.; Elmaci, Y. Aroma characterization of virgin olive oil from two Turkish olive varieties by SPME/GC/MS. *Int. J. Food Prop.* **2011**, *14*, 1160–1169. [CrossRef]
22. Reboredo-Rodríguez, P.; González-Barreiro, C.; Cancho-Grande, B.; Simal-Gándara, J. Dynamic headspace/GC–MS to control the aroma fingerprint of extra-virgin olive oil from the same and different olive varieties. *Food Control.* **2012**, *25*, 684–695. [CrossRef]
23. García-Vico, L.; Belaj, A.; Sánchez-Ortiz, A.; Martínez-Rivas, J.M.; Pérez, A.G.; Sanz, C. Volatile compound profiling by HS-SPME/GC-MS-FID of a core olive cultivar collection as a tool for aroma improvement of virgin olive oil. *Molecules* **2017**, *22*, 141. [CrossRef] [PubMed]
24. The Good Scents Company. The Good Scents Company Information System. Available online: <http://www.thegoodscentscompany.com/data/rw1038291.html> (accessed on 3 September 2021).

25. Da Costa, J.R.O.; Dal Bosco, S.M.; Ramos, R.C.d.S.; Machado, I.C.K.; Garavaglia, J.; Villasclaras, S.S. Determination of volatile compounds responsible for sensory characteristics from Brazilian extra virgin olive oil using HS-SPME/GC-MS direct method. *J. Food Sci.* **2020**, *85*, 3764–3775. [[CrossRef](#)] [[PubMed](#)]
26. Ciurczak, E.W.; Igne, B.; Workman, J., Jr.; Burns, D.A. *Handbook of Near-Infrared Analysis*; CRC Press: Boca Raton, FL, USA, 2021.
27. Borghi, F.T.; Santos, P.C.; Santos, F.D.; Nascimento, M.H.; Correa, T.; Cesconetto, M.; Pires, A.A.; Ribeiro, A.V.; Lacerda, V., Jr.; Romao, W. Quantification and classification of vegetable oils in extra virgin olive oil samples using a portable near-infrared spectrometer associated with chemometrics. *Microchem. J.* **2020**, *159*, 105544. [[CrossRef](#)]
28. Burns, D.A.; Ciurczak, E.W. *Handbook of Near-Infrared Analysis*; CRC Press: Boca Raton, FL, USA, 2007.
29. Cayuela, J.A.; García, J.F. Nondestructive measurement of squalene in olive oil by near infrared spectroscopy. *LWT* **2018**, *88*, 103–108. [[CrossRef](#)]
30. Pineda, M.; Rojas, M.; Gálvez-Valdivieso, G.; Aguilar, M. The origin of aliphatic hydrocarbons in olive oil. *J. Sci. Food Agric.* **2017**, *97*, 4827–4834. [[CrossRef](#)] [[PubMed](#)]
31. Giuffrè, A.M. The effect of cultivar and harvest season on the n-alkane and the n-alkene composition of virgin olive oil. *Eur. Food Res. Technol.* **2021**, *247*, 25–36. [[CrossRef](#)]
32. Moret, S.; Populin, T.; Conte, L.S. Mineral paraffins in olives and olive oils. In *Olives and Olive Oil in Health and Disease Prevention*; Elsevier: Amsterdam, The Netherlands, 2010; pp. 499–506.
33. Fountoulakis, M.; Drakopoulou, S.; Terzakis, S.; Georgaki, E.; Manios, T. Potential for methane production from typical Mediterranean agro-industrial by-products. *Biomass Bioenergy* **2008**, *32*, 155–161. [[CrossRef](#)]
34. Del Alamo, R.R.; Fregapane, G.; Aranda, F.; Gómez-Alonso, S.; Salvador, M. Sterol and alcohol composition of Cornicabra virgin olive oil: The campesterol content exceeds the upper limit of 4% established by EU regulations. *Food Chem.* **2004**, *84*, 533–537. [[CrossRef](#)]